A High-Q Broad-Band Active Inductor and Its Application to a Low-Loss Analog Phase Shifter

Hitoshi Hayashi, *Member, IEEE*, Masahiro Muraguchi, *Member, IEEE*, Yohtaro Umeda, *Member, IEEE*, and Takatomo Enoki, *Member, IEEE*

***Abstract*—This paper demonstrates a high-Q broad-band active inductor and its application to a low-loss analog phase shifter. The proposed high-Q broad-band active inductor utilizes frequency-insensitive negative resistance to compensate constant internal losses caused by the drain-to-source conductance of the field-effect transistors (FET's), the dc bias circuit, and several other factors. The measured frequency range of the fabricated InAlAs/InGaAs/InP HEMT active inductor is 6 to 20 GHz for Q values greater than 100, and 7 to 15 GHz for Q values greater than 1000. A low-loss analog phase shifter is also fabricated at C-band. This is constructed with the active inductors, the varactor diodes and the low-loss multilayer broad-side coupler in a MIC structure. Since the constant negative resistance of the active inductors also compensates the line loss of the coupler and the varactor diodes' series resistance, the measured results show a good insertion loss performance with a large phase shift. A phase shift of more than 225° within a 0.8 dB insertion loss from 4.7 to 6.7 GHz, another of more than 180° within 1.3 dB insertion loss from 3.7 to 8.5 GHz, and one more of more than 90° within 1.4 dB insertion loss from 3.5 to 10.6 GHz were obtained.**

I. Introduction

IN MONOLITHIC microwave integrated circuits (MMIC's), spiral inductors are often used for generating inductance because of their simple structure. However, to generate a lot of inductance, large spiral inductors are needed which take up too much space. Field-effect transistors (FET's) utilize space more effectively, which has called attention to their potential use as active inductors [1]–[6]. However, the significant constant internal loss due to their drain-to-source conductance, the resistors for dc bias, and the dc bias circuit all inevitably degrade the performance of active inductors [1]. Several approaches to solve these problems have been introduced, including some promising ones that achieve high-Q values by using negative resistance. However, even these techniques result in limited band characteristics, and the experimental active inductor's bandwidth for Q values greater than 50 was 30–40%. As indicated by Hara *et al.s'* experiments, this is probably because the internal loss—caused by the drain-to-source conductance of the FET's, the resistors for dc bias, and several other factors—are almost constant at the operating frequency range below half of the cut-off frequency [1]. On the other hand, the negative resistance of Hara *et al.s'* inductor is parallel to inductance, and that of Alinikula *et al.s'* inductor is in series with inductance but not constant against the operating frequency range [7]. If the negative resistance generated in series with the inductance could be made constant against the operating frequency, the loss could be canceled over a much wider frequency band, i.e., from dc to the microwave frequency range.

We fabricated high-Q broad-band active inductors in which the circuit structure generates frequency-insensitive negative resistance that almost completely compensates the constant internal loss. This yields a much wider frequency band than offered with previously reported active inductors. This paper describes our active inductors and experimental results.

The paper also describes a low-loss analog reflection-type phase shifter that we fabricated in a microwave integrated circuit (MIC) structure. Bastida *et al.* demonstrated a hybrid 180° reflection-type phase shifter as an application of the active inductors. In this case, the active inductors were used as tuning inductive elements. The insertion loss was modest (less than 3.8 dB in the 2.3–4.6 GHz band) because the inductors used common-source cascode FET's with resistive feedback lossy topology. Since the constant negative resistance of the proposed active inductor can compensate the internal loss of the coupler and the varactor diodes' series resistance effectively, the internal loss of the phase shifter could be low over the broad-band frequency range. To the best of our knowledge there are no reports on the application of active inductors to the phase shifter to reduce internal loss, although there are reports on the implementation of negative resistance elements to compensate for losses in microwave active filters [8]–[11].

II. Novel Active Inductor

A. Design Approach

A schematic of the active inductor we propose is shown in Fig. 1(a). This circuit is composed of common-source cascode FET's (FET_1 and FET_2) and a feedback FET (FET_3). Hara *et al.* used a configuration for the active inductor in which FET_3 was a common-gate FET [1]. More recently, a technique has been developed in which a resistor is inserted in the gate of a common-gate FET to generate negative resistance in series with inductance but not constant against the operating frequency range [7]. In our new active inductor, the gate of FET_3 is connected to the drain of FET_1 and the source of FET_2. This connection enables the active inductor to generate constant series negative resistance. In addition, a resistor R_{out}

Manuscript received April 2, 1996.

The authors are with NTT Wireless Systems Laboratories, Kanagawa 238-03, Japan.

Publisher Item Identifier S 0018-9480(96)08714-5.

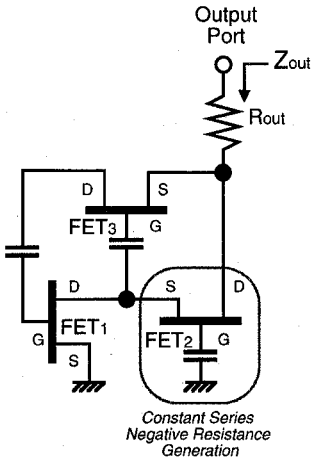

(a)

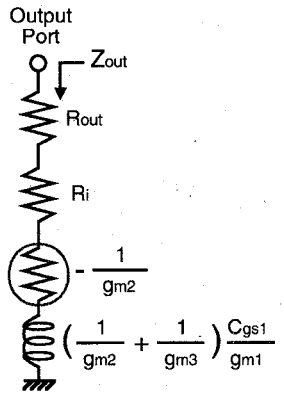

(b)

Fig. 1. Basic configuration of proposed active inductor using constant series negative resistance generation: (a) circuit schematic, (b) simplified equivalent circuit.

is inserted between the drain of FET2 and the output port. It has been shown that the internal loss R_i, caused by the drain-to-source conductance of the FET's, the resistors for dc bias, and several other factors, is almost constant at the operating frequency range below half of the cut-off frequency [1]. If the FET equivalent circuit is assumed to be just a combination of the transconductance g_m and the gate-to-source capacitance C_{gs}, the output impedance, Z_{out}, is as shown in (1), at the bottom of the page.

When the FET's have the same cut-off frequency f_T ($= g_m/2\pi C_{gs}$), (1) can be rewritten as follows:

$$Z_{\text{out}} = \frac{\frac{j\omega C_{gs1}}{g_{m_1}}\left(\frac{1}{g_{m_2}}+\frac{1}{g_{m_3}}\right)-\frac{1}{g_{m_2}}}{1-\left(\frac{f}{f_T}\right)^2}+R_{\text{out}}. \tag{2}$$

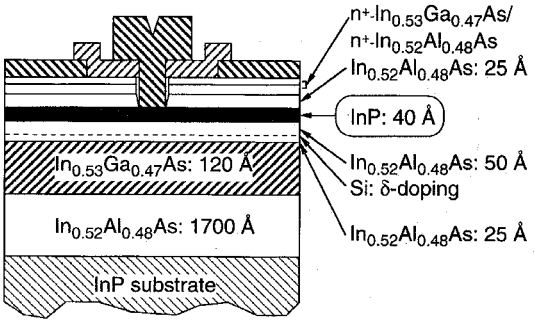

Fig. 2. Structure of an InAlAs/InGaAs/InP HEMT with an InP recess-etch stopper.

Assuming that

$$(f/f_T)2 \ll 1 \tag{3}$$

we have a simplified equivalent circuit as shown in Fig. 1(b). Note that the negative resistance shows no frequency term so R_i can be completely canceled by adjusting the amounts of R_{out} and g_{m_2} for the entire frequency range. It also shows in (2) that this circuit has a higher inductance value than previously reported circuits [7].

Since FET1, FET2, and FET3 draw the same drain current in this configuration, it is difficult to control the inductance and the negative resistance independently. One method to obtain a tunable active inductor is to use a cold-FET variable resistor as the resistor R_{out} for tuning the series negative resistance. Then g_{m_2} or g_{m_3} could be varied for tuning the inductance, while maintaining series resistance constant with the cold-FET variable resistor R_{out}.

B. Experimental Results

The high-Q broad-band active inductor was fabricated using four 0.1-μm-gate-length InAlAs/InGaAs/InP high electron mobility transistors (HEMT's) [12]. InAlAs/InGaAs modulation-doped heterostructure lattice matched to InP substrate was grown by metal-organic chemical vapor deposition for the HEMT's. Fig. 2 shows the cross section of the HEMT. An InP layer was inserted in the InAlAs barrier layer as a gate-recess-etch stopper to make the depth of the gate recess uniform. The InP etching stopper is compatible with the n^+-InGaAs/n^+-InAlAs cap layer used for nonalloyed ohmic contact in the fabrication process. The HEMT's showed a very high average f_T and $f_{\max}$ of 140 and 180 GHz, respectively.

The circuit schematic of the active inductor that we fabricated is shown in Fig. 3(a). FET4 is used for dc biasing. The fixed resistor Rout is 29 Ω. The size of the chip shown in the photograph in Fig. 3(b) is 0.78 × 0.4 mm^2. Since the MMIC structure uses 'uniplanar' techniques based on the

$$Z_{\text{out}} = \frac{\frac{j\omega C_{gs1}}{g_{m_1}}\left\{\frac{1}{g_{m_2}}+\frac{1}{g_{m_3}}\frac{\left(1+\frac{j\omega C_{gs2}}{g_{m_2}}\right)}{\left(1+\frac{j\omega C_{gs3}}{g_{m_3}}\right)}\right\}-\frac{1}{g_{m_2}}\left\{1+\frac{\left(\frac{j\omega C_{gs1}}{g_{m_1}}-\frac{j\omega C_{gs3}}{g_{m_3}}\right)}{\left(1+\frac{j\omega C_{gs3}}{g_{m_3}}\right)}\right\}}{1-\frac{\omega C_{gs1}}{g_{m_1}}\frac{\omega C_{gs3}}{g_{m_3}}\frac{\left(1+\frac{j\omega C_{gs2}}{g_{m_2}}\right)}{\left(1+\frac{j\omega C_{gs3}}{g_{m_3}}\right)}-\frac{j\omega C_{gs1}}{g_{m_1}}\left\{1-\frac{\left(1+\frac{j\omega C_{gs2}}{g_{m_2}}\right)}{\left(1+\frac{j\omega C_{gs3}}{g_{m_3}}\right)}\right\}+\frac{\left(\frac{j\omega C_{gs1}}{g_{m_1}}-\frac{j\omega C_{gs3}}{g_{m_3}}\right)}{\left(1+\frac{j\omega C_{gs3}}{g_{m_3}}\right)}}+R_{\text{out}} \tag{1}$$

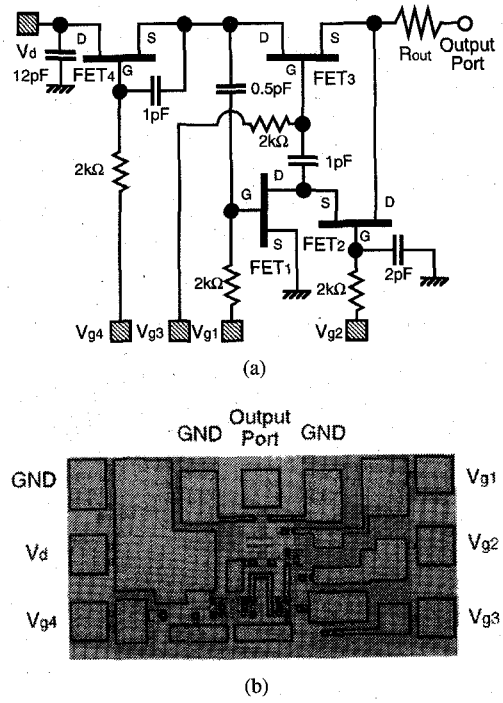

Fig. 3. Fabricated active inductor: (a) circuit schematic and (b) photograph of MMIC chip.

coplanar waveguide, it is important that the metal surrounding the inductor's circuit is sufficiently grounded to ensure high-Q characteristics at the higher frequency range [13].

Fig. 4 shows S parameters (from 2 to 26 GHz) measured using the Cascade Microtech Summit 10 600 semi-automatic thermal probing system. The associated series resistance is kept above 0 Ω in the frequency range 0.045–26.5 GHz by the appropriate bias conditions, $V_{g1} = 0.0$ V, $V_{g2} = 1.2$ V, $V_{g3} = 2.4$ V, $V_{g4} = 3.5$ V, $V_d = 4.9$ V, and $I_d = 11$ mA. This corresponds to a power consumption of 54 mW, and shows that loss can be compensated at up to and over 20 GHz. The measured S parameters at 2 GHz are capacitive because of the small value of the dc cut capacitors, which are not considered in the simplified analysis above. Fig. 5 shows the measured impedance-frequency characteristics, where the impedance is represented by series resistance and inductance. The inductance values at 6 GHz and 20 GHz are respectively 0.41 nH and 0.82 nH, and the Q value in this frequency range is greater than 100. The inductance values at 7 GHz and 15 GHz are respectively 0.44 nH and 0.59 nH, and the Q value in this frequency range is greater than 1000. The low-loss and wide-band characteristics are due to the proposed constant series negative resistance compensation.

Considering applications for active filters, phase shifters, oscillators and so forth, one of the most important problems is stability against temperature variation. The temperature variation from −5° to 55°C was measured [7]. The variation of the inductance and resistance values is within 6.2 % and 1.4 Ω, respectively, at the frequency of 8 GHz. The variation of the resistance is almost flat over the 4–18 GHz frequency band, because the amount of negative resistance varies constant in proportion with the temperature variation against the operating frequency range.

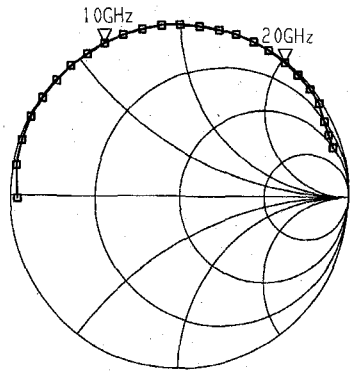

Fig. 4. Measured S parameters of the experimental circuit.

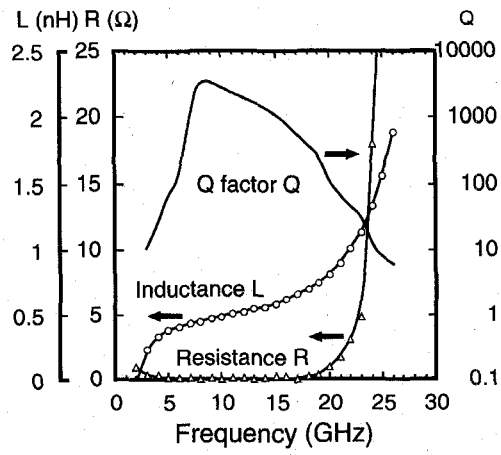

Fig. 5. Measured impedance-frequency characteristics of the experimental active inductor.

The input-output characteristics at the frequency of 8 GHz was measured to investigate dynamic range as shown in Fig. 6. An 8-GHz signal was injected into the active inductor through a circulator, and the reflected signal was observed by a spectrum analyzer [7]. The 1-dB gain compression point is −1 dBm of incident power, and the fundamental power to the second-harmonic wave power of the reflected signal is more than 20 dB. The phase deviation is less than 1° in this incident power range, which means that the variation of the inductance and resistance values are negligible up to −1 dBm of input power. It has been shown that the AM-PM conversion characteristics of the common-source cascode FET amplifier are good because the positive phase deviation from the common-source FET and the negative phase deviation from the common-gate FET at the near saturation region cancel each other [14]. Since in our active inductor the common-source FET (FET1) is connected to the common-gate FET (FET2), the good AM–PM conversion characteristics are thought to be due to the same reason.

III. Low-Loss Analog Phase Shifter

A. Design Approach

The basic topology of the proposed phase shifter is illustrated in Fig. 7. The 3-dB, 90° hybrid divides the input signal from port #1 equally between the two output ports, port #3 and port #4, but with a difference of 90°. Port #3 and port #4 are terminated with the same reactance circuits. Signals

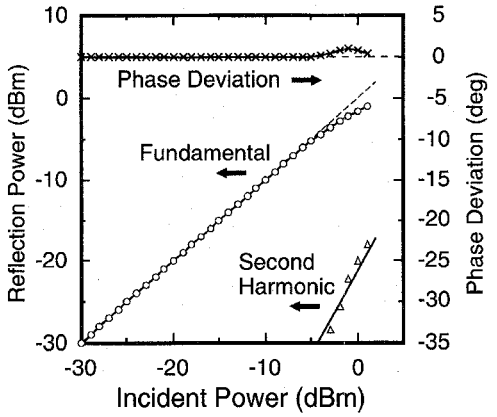

Fig. 6. Reflection power and phase deviation versus incident power.

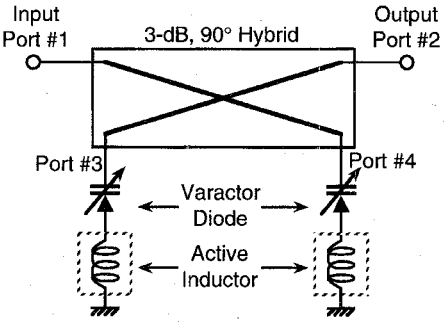

Fig. 7. Basic topology of the proposed phase shifter.

reflected back from the port #3 and port #4 are added together at port #2, and no signal returns to port #1. The phase shift is determined by the reactance values at port #3 and port #4.

Compared to conventional analog reflection-type phase shifters, the reactance circuits of the new phase shifters are constructed with the varactor diodes connected in series to the active inductors. The varactor diodes are used as tuning elements just like in the conventional phase shifters [15]. The active inductors are used to reduce the loss of the phase shifter by generating constant negative resistance against the operating frequency range. In Section II-A, we mentioned that the internal loss R_i of the active inductor can be completely canceled by adjusting the amounts of R_{out} and g_{m_2}. It is necessary to modify these design parameters in order to compensate not only the internal loss R_i but also the line loss of the coupler and the varactor diode's series resistance.

In the conventional phase shifter using the passive inductor, not only the loss of the inductor but also the line loss of the coupler and the varactor diode's resistance increase the insertion loss. Furthermore, the loss causes a large amount of the amplitude variation with the phase shift operation, especially if a series, a parallel, or a combination series-parallel resonant circuit is used as a reactance circuit in order to obtain a large phase shift. If a lossless reactance circuit is used in the phase shifter, a quasiideal phase shifter, in which the insertion loss is constantly zero with the phase shift operation, is obtained.

B. Multilayer Broad-Side Coupler

Recently, multilayer MMIC technology has been developed to reduce chip size for better performing MMIC's [16], [17].

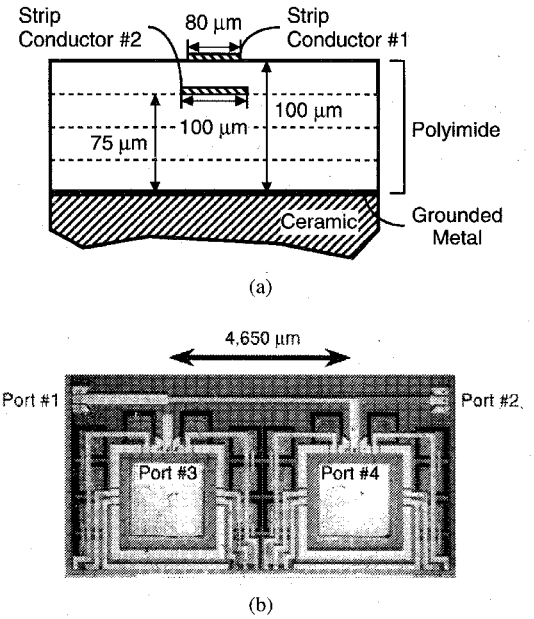

Fig. 8. Multilayer broad-side coupler: (a) cross-sectional view and (b) photograph of chip.

In this technology, thin polyimide films and conductors are stacked on the surface of the active devices to fabricate passive circuits. However, the metal lines of these structures are relatively lossy because the thickness of the metal is about 1–2 μm.

We fabricated a low-loss multilayer broad-side coupler used in a MIC structure as shown in Fig. 8. Although four layers of the ceramic and the polyimide are stacked in this substrate, only the polyimide layers are used for the broad-side coupler. Each polyimide layer is 25-μm thick. The strip conductor and the grounded metal between the polyimide layer and ceramic layer have a thickness of 5 μm and are made of gold. The polyimide layer has the following characteristics: the relative dielectric constant, ε_r, is 3.2; the dielectric loss tangent, $\tan\delta$, is 0.002; and the coefficient of heat expansion is 50×10^{-6}/°C at the frequency of 10 GHz. The broad-side coupler is fabricated by stacking two strip conductors, which are respectively located at heights of 75 μm and 100 μm from the grounded metal. The respective widths of strip conductors #1 and #2 are 80 μm and 100 μm, and the length of the coupler is 4,650 μm. This structure effectively provides a tight coupling (3 dB) between the strip conductors.

Fig. 9 shows the measured performance of the broad-side coupler. A coupling loss of 3.4 ± 0.7 dB, and a return loss and isolation of more than 16 dB have been obtained over the 5.4–13.3 GHz frequency band. The phase difference between the two ports, port #3 and port #4 was within $90 \pm 2°$ in the same frequency range. The mean coupling loss is about 1.6 dB lower than that of the previously reported multilayer MMIC broad-side coupler [17]. This is due to the wide and thick metal conductors of the fabricated multilayer structure.

C. Experimental Results of the Phase Shifter

Fig. 10 shows a photograph of the MIC phase shifter. The varactor diodes are mounted on the coupler's ports. The

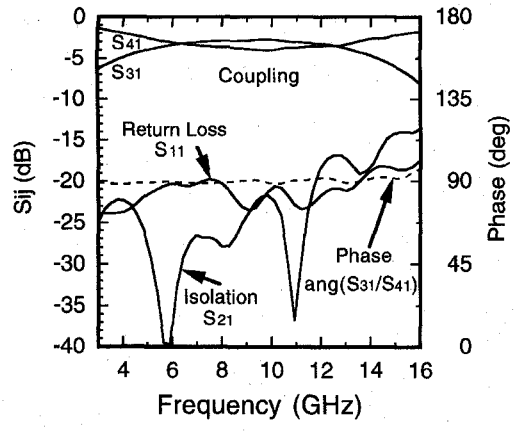

Fig. 9. Measured performance of the broad-side coupler.

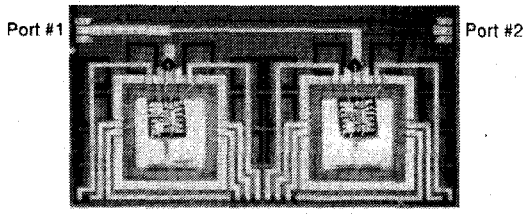

Fig. 10. Photograph of the MIC phase shifter.

MMIC's mentioned in Section II-B sit on the surface of the grounded metal between the ceramic and polyimide layers and are connected to the varactor diodes by 20 μm$\emptyset$ Au bonding wires. The chip size is 9.3 mm $\times$ 4.8 mm.

Two hyper-abrupt GaAs variable capacitance diodes (SANYO SVD-201) were employed as varactor diodes. The series resistance, R_s, and capacitance, C_j, at the reverse bias voltage of 0 V are, respectively, 3 Ω and 1.8 pF at 10 GHz. The capacitance ratio between the reverse bias voltage of 0 V to 12 V is about 11:1.

Fig. 11 shows measured insertion loss and return loss at the varactors' bias voltage, V_c, of 0.6 V. The biases of the active inductors are set so that the insertion loss is as low as possible at all frequency ranges. The measured insertion loss is within 0.8 dB across the 3.6 to 12.1 GHz frequency range. The measured input return loss is more than 10 dB in the same frequency range. This modest input match is attributed to the MIC structure and the difference of the electrical characteristics of the two active inductors and varactor diodes. Of course, it could be that the active inductors are operating in a reflection-type amplifier mode, and the positive gain could be achieved by varing the biases of the active inductor. However, the return loss performance would degrade.

Fig. 12 shows the measured relative phase shift and insertion loss with varying V_c. The reference phase is at V_c of 0.6 V. A maximum relative phase shift of 231° was achieved at 5.7 GHz by changing V_c to 11.6 V.

The phase shifts obtained by changing V_c to 11.6 V are as follows: 1) a phase shift of more than 225° within 0.8 dB insertion loss from 4.7 to 6.7 GHz, 2) a phase shift of more than 180° within 1.3 dB insertion loss from 3.7 to 8.5 GHz, and 3) a phase shift of more than 90° within 1.4 dB insertion loss from 3.5 to 10.6 GHz.

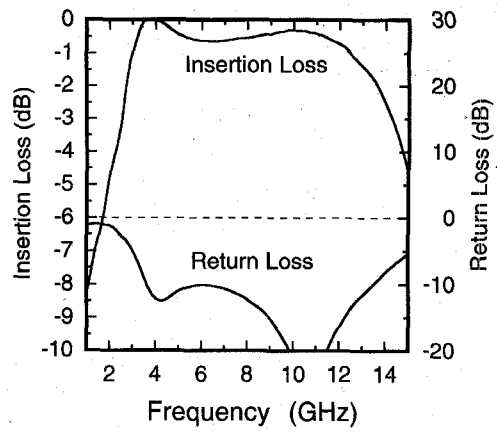

Fig. 11. Measured insertion loss and return loss at V_c of 0.6 V.

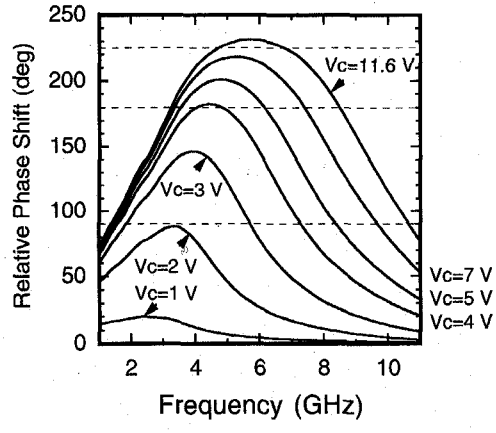

(a)

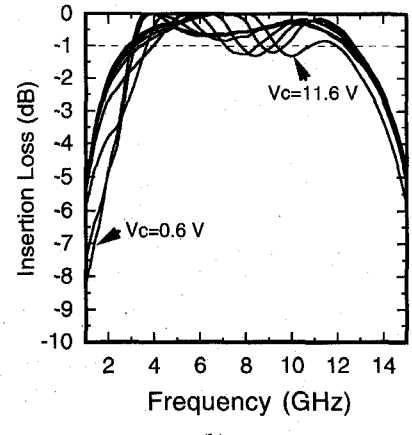

(b)

Fig. 12. Measured relative phase shift and insertion loss with varying V_c: (a) relative phase shift and (b) insertion loss.

The phase shift errors obtained are as follows: 1) for a phase shift of 225°, the error was ±2° within 0.8 dB insertion loss from 4.8 to 6.3 GHz obtained by changing V_c to 9 V and 2) for a phase shift of 180°, the error was ±3° within 1 dB insertion loss from 3.9 to 5 GHz obtained by changing V_c to 4 V.

Since the phase shifter uses a large number of active elements, the noise figure performance was relatively poor [3]. The measured noise figure at 5 GHz was 9.1 dB at V_c of 4 V.

In this experiment, only the varactor diodes were tunable. If the tunable active inductors discussed in Section II are used,

then the results will be even better because the amount of the phase shift will be the sum of the two individual tuning ranges attributed to the tunable active inductors and varactor diodes.

IV. Conclusion

A high-Q broad-band active inductor and its application to a low-loss analog reflection-type phase shifter was demonstrated. The proposed high-Q broad-band active inductor utilizes the frequency-insensitive negative resistance to compensate constant internal losses resulting from drain-to-source conductance of the FET's and the dc bias circuit, and so forth. The measured frequency range of the fabricated InAlAs/InGaAs/InP HEMT active inductor was 6 to 20 GHz for Q values greater than 100, and 7 to 15 GHz for Q values greater than 1,000. This inductor is excellent for high-performance filters, VCO's and analog phase shifters. To demonstrate its application, active inductors were used in a low-loss reflection-type analog phase shifter at C-band. This was constructed with the active inductors, varactor diodes and a low-loss multilayer broad-side coupler in the MIC structure. Since the constant negative resistance of the active inductor also compensates the line loss of the coupler and the varactor diode's series resistance, our measured results showed a good insertion loss performance, with a large phase shift. We obtained a phase shift of more than 225° within 0.8 dB insertion loss from 4.7 to 6.7 GHz, another of more than 180° within 1.3 dB insertion loss from 3.7 to 8.5 GHz, and one more of more than 90° within 1.4 dB insertion loss from 3.5 to 10.6 GHz.

Acknowledgment

The authors would like to thank A. Hashimoto and Dr. K. Kohiyama for their helpful information and encouragement.

References

[1] S. Hara, T. Tokumitsu, and M. Aikawa, "Lossless broad-band monolithic microwave active inductors," *IEEE Trans. Microwave Theory Tech.*, vol. 37, pp. 1979–1984, Dec. 1989.

[2] G. F. Zhang, M. L. Villegas, and C. S. Ripoll, "New broadband tunable monolithic microwave floating active inductor," *Electron. Lett.*, vol. 28, no. 1, pp. 78–81, 1992.

[3] C. Zanchi, T. Parra, and J. Graffeuil, "A tunable lossless HBT broad-band monolithic microwave floating active inductor," in *Proc. 24th EuMC*, 1994, pp. 793–798.

[4] P. Alinikula, R. Kaunisto, and K. Stadius, "Monolithic active resonators for wireless applications," in *IEEE Microwave and Millimeter-Wave Monolithic Circuits Symp. Dig.*, 1994, pp. 197–200.

[5] S. Lucyszyn and I. D. Robertson, "Monolithic narrow-band filter using ultrahigh-Q tunable active inductors," *IEEE Trans. Microwave Theory Tech.*, vol. 42, pp. 2617–2622, Dec. 1994.

[6] E. M. Bastida, G. P. Donzelli, and L. Scopelliti, "GaAs monolithic microwave integrated circuits using broadband tunable active inductors," in *Proc. 19th EuMC*, 1989, pp. 1282–1287.

[7] H. Hayashi, M. Muraguchi, Y. Umeda, and T. Enoki, "A novel loss compensation technique for high-Q broad-band active inductors," in *IEEE Microwave and Millimeter-Wave Monolithic Circuits Symp. Dig.*, June 1996, pp. 103–106.

[8] C. Chang and T. Itoh, "Monolithic active filters based on coupled negative resistance method," *IEEE Trans. Microwave Theory Tech.*, vol. 38, pp. 1879–1884, Dec. 1990.

[9] B. Hopf and I. Wolff, "Narrow band MMIC active filter using negative resistance circuits in coplanar line technique," in *Proc. 25th EuMC*, 1995, pp. 1110–1112.

[10] T. Nishikawa, Y. Ishikawa, J. Hattori, and K. Wakino, "Dielectric receiving filter with sharp stopband using an active feedback resonator method for cellular base stations," *IEEE Trans. Microwave Theory Tech.*, vol. 37, pp. 2074–2079, Dec. 1989.

[11] P. Katzin, B. Bedard, and Y. Ayasli, "Narrow-band MMIC filters with automatic tuning and Q-factor control," in *IEEE Microwave and Millimeter-Wave Monolithic Circuits Symp. Dig.*, June 1993, pp. 141–144.

[12] T. Enoki, H. Ito, K. Ikuta, and Y. Ishii, "0.1-μm InAlAs/InGaAs HEMT's with an InP-recess-etch stopper grown by MOCVD," in *IEEE 7th Int. Conf. on InP and Related Materials Dig.*, Sapporo, Japan, 1995, pp. 81–84.

[13] M. Muraguchi, T. Hirota, A. Minakawa, K. Ohwada, and T. Sugeta, "Uniplanar MMIC's and their applications," *IEEE Trans. Microwave Theory Tech.*, vol. 36, pp. 1896–1901, 1988.

[14] H. Hayashi, M. Nakatsugawa, and M. Muraguchi, "Quasi-linear amplification using self phase distortion compensation technique," *IEEE Trans. Microwave Theory Tech.*, vol. 43, pp. 2557–2564, Nov. 1995.

[15] C. L. Chen, W. E. Courtney, L. J. Mahoney, M. J. Manfra, A. Chu, and H. A. Atwater, "A low-loss Ku-band monolithic analog phase shifter," *IEEE Trans. Microwave Theory Tech.*, vol. 35, pp. 315–320, Mar. 1987.

[16] H. Nakamoto, T. Tokumitsu, and M. Akaike, "A monolithic, port-interchanged rat-race hybrid using a thin-film microstrip line crossover," in *Proc. 19th EuMC*, 1989, pp. 311–316.

[17] I. Toyoda, T. Hirota, T. Hiraoka, and T. Tokumitsu, "Multilayer MMIC branch-line coupler and broad-side coupler," in *IEEE Microwave and Millimeter-Wave Monolithic Circuits Symp. Dig.*, June 1992, pp. 79–82.

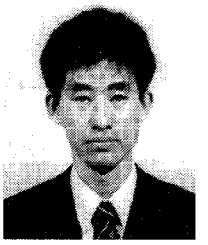

Hitoshi Hayashi (M'94) was born in Nagoya, Japan, in 1966. He received the B.E. and M.E. degrees in electronics engineering from the University of Tokyo, Tokyo, Japan, in 1990 and 1992, respectively.

In 1992, he joined NTT Radio Communication Systems Laboratories, Yokosuka, Japan, and since then he has been involved in research on GaAs MMIC's. He is currently at NTT Wireless Systems Laboratories, Yokosuka, Japan, where he is engaged in the development of microwave amplifiers.

Mr. Hayashi is a member of the Institute of Electronics, Information and Communication Engineers (IEICE) of Japan.

Masahiro Muraguchi (S'80-M'83) was born in Kanazawa, Japan, on May 23, 1955. He received the B.S. degree in electrical engineering from the Nagoya Institute of Technology in 1978 and the M.S. and Ph.D degrees in physical electronics engineering from the Tokyo Institute of Technology in 1980 and 1983, respectively.

He jointed the NTT Atsugi Electrical Communications Laboratories, Nippon Telegraph and Telephone Corporation, in 1983, where he was involved in the design and fabrication of GaAs MMIC's. He is currently engaged in research and development work on MMIC's for wireless communications at the NTT Wireless Systems Laboratories, Yokosuka, where he is currently the leader of the Microwave Circuit Group.

Dr. Muraguchi was awarded the Ichimura Prize by the New Technology Development Foundation in 1994. He has been on the Editorial Committee of *IEICE Transactions on Electronics* as an Associate Editor since 1994. He is a member the Institute of Electronics, Information and Communication Engineers (IEICE) of Japan.

Yohtaro Umeda (M'89), for a photograph and biography, see this issue, p. 2368.

Takatomo Enoki (M'91), for a photograph and biography, see this issue, p. 2368.